Violation of the Zener power law for linear magnetostriction in the weak random anisotropy $Tb_xY_{1-x}Al_2$ magnets



1996 J. Phys.: Condens. Matter 8 6945

(http://iopscience.iop.org/0953-8984/8/37/016)

J. Phys.: Condens. Matter **8** (1996) 6945–6955. Printed in the UK

# Violation of the Zener power law for linear magnetostriction in the weak random anisotropy $Tb_xY_{1-x}Al_2$ magnets

A del Moral, C de la Fuente and J I Arnaudas

Magnetismo de Sólidos, Departamento de Física de Materia Condensada and Instituto de Ciencia de Materiales de Aragón, Universidad de Zaragoza and Consejo Superior de Investigaciones Científicas, 50009 Zaragoza, Spain

Received 20 March 1996, in final form 30 May 1996

**Abstract.** The linear magnetostriction $\lambda_2$ has been measured in the $Tb_xY_{1-x}Al_2$ intermetallic compounds. The Zener power law, which gives $\lambda_2$ as proportional to the third power $m^3$ of the reduced magnetization, is found to be valid in the ferromagnetic phase of $TbAl_2$. For $x < 1$ the compounds are weak random anisotropy magnets, and in the quasisaturated regime induced by a magnetic field $\lambda_2$ is still proportional to $m^p$, but the exponent $p$ is smaller than three. $p$ increases with the field and approaches three in the high-field limit (12 T). A relation between the violation of the Zener power law and the reduction of the magnetization in the random anisotropy systems is derived, and is compared with the experimental results.

## 1. Introduction

For ferromagnets Zener's $n(n+1)/2$ power law of linear magnetostriction [1], $\lambda_n$, where $n$ is an even integer, relates the reduced magnetostriction $\lambda_n(T, H)/\lambda_n(0, H)$ at temperature $T$ and applied magnetic field $H$ to the reduced magnetization $m(T, H) \equiv M(T, H)/M(0, H) = \langle J_z\rangle_T/\langle J_z\rangle_0$ in the well known form [2]

$$\lambda_n(T, H)/\lambda_n(0, H) = m(T, H)^{n(n+1)/2}. \tag{1}$$

$n$ is the order of the quantum spherical harmonic $Y_n^0(\boldsymbol{J})$ (or Stevens' operator $O_n^0(\boldsymbol{J})$ and $\boldsymbol{J}$ the ionic total angular momentum, with projection $J_z$ along the quantization axis. This law, valid at low enough temperatures, is of *extreme* generality, only requiring single-ion anisotropy of crystal electric field (CEF) origin, localized magnetic moments and ionic low energy levels equally spaced [3]. It appears because of the relationship found between the averages $\langle Y_n^0(\boldsymbol{J})\rangle_T$ and $\langle Y_1^0(\boldsymbol{J})\rangle_T \equiv \langle J_z\rangle_T$, when the quantization axis is rotated to coincide with the sample average magnetization [2], $\boldsymbol{M}$, and the ionic $\boldsymbol{J}$ angular momentum distribution around the $\boldsymbol{M}$ direction is assumed to have cylindrical symmetry [1]. $\langle\ldots\rangle_T$ is the canonical thermal average, i.e. $\langle\ldots\rangle_T = \mathrm{Tr}(\rho Y_n^0)/\mathrm{Tr}\,\rho$, where $\rho(T, H)$ is the density matrix. This law applies to any irreducible magnetostrictive strain of a crystal or to the linear (also called anisotropic) magnetostriction in polycrystalline samples. Although such a relation derives from a particular feature within the mean-field approximation, it can be shown that the same result is obtained in all quasi-independent collective excitation theories and within the framework of the one-particle density matrix, as appearing in Green function theories [4]. One of those theories is, indeed, the spin wave approximation, used in this work.

0953-8984/96/376945+11$19.50  

Usually the strongest contribution to the measured magnetostrictive irreducible strains in crystals or to the linear magnetostriction in polycrystalline samples is the $n = 2$ or second-order striction and therefore we will focus our attention on it. Then we have

$$\lambda_2(T, H)/\lambda_2(0, H) = \langle Y_2^0(\boldsymbol{J})\rangle_T/\langle Y_2^0(\boldsymbol{J})\rangle_0 = m^3(T, H) \tag{2}$$

where $Y_2^0(\boldsymbol{J}) = 3J_z^2 - J(J+1)$. It should be clearly stated that (1) and (2) are only valid for good 3D Heisenberg ferromagnets, with localized moments.

Recently much work has been done on linear magnetostriction for magnetically disordered amorphous alloys, based both on magnetic transition metals and on rare earths (REs) [5]. However for the key case (as we shall see) of crystalline disorderly diluted (by a nonmagnetic partner such as Y, Sc, La or Lu) RE intermetallic compounds such information is not available. It seems natural to look for some kind of Zener-like law for them. Elsewhere [6] we have presented an early version of a model for linear magnetostriction in disordered quasiferromagnets, which predicts $p$ exponents which can be rather smaller than three. This happens in fact for magnets having a random distribution of local easy magnetization axes, i.e. for the random magnetic anisotropy (RMA) magnets. This prediction is now exposed in greater detail and tested with available magnetostriction data for the intermetallic Laves phase pseudobinaries $Tb_xY_{1-x}Al_2$. The crystalline character of our systems is the mentioned key point: to dispose of a reference compound where $p = 3$, i.e. $TbAl_2$, which is a good 3D Heisenberg ferromagnet with $\langle 111\rangle$ easy direction and $T_c = 103$ K [7]. A good many experimental probes and magnetic measurements [8] have shown that the $Tb_xY_{1-x}Al_2$ series depicts weak RMA. The magnetic phase diagram [8] shows the presence of paramagnetic (P), spin glass (SG) and correlated spin glass (CSG) phases, with the triple point at $x_{tr} = 0.27$ and $T_{tr} = 8.6$ K, above which the SG is reentrant into the CSG phase, up to about $x = 0.5$, where it seems to collapse.

A good descriptive Hamiltonian for localized moment RMA systems is that of Harris and coworkers [9],

$$H = -(1/2)J_0(g_J - 1)^2 \sum_{l\neq l'} \boldsymbol{J}_l \cdot \boldsymbol{J}_{l'} - D\sum_l (\hat{\boldsymbol{a}}_l \cdot \boldsymbol{J}_l)^2 - g_J\mu_B \boldsymbol{H} \cdot \sum_l \boldsymbol{J}_l \tag{3}$$

where $J_0$ is the effective spin exchange interaction, $D$ the local CEF strength, $\hat{\boldsymbol{a}}_l$ the local easy axis at site $\boldsymbol{l}$, $g_J$ the Landé factor and $\boldsymbol{H}$ the applied magnetic field. For $RE_xY_{1-x}Al_2$ (RE = Dy, Tb) magnets the RMA can have different origins [10]. The most likely is through the following magneto-elastic coupling (MEC) amplifying effect. Random substitutions of the smaller radius $Y^{3+}$ ions will produce cubic symmetry distorting local strains, which coupled to $\boldsymbol{J}$ through the MEC will give rise to an axial CEF of random direction gradient. The estimated $D/J_0$ ratio from this source is $\cong 0.04$ [8, 10]. Other possible sources of RMA are the difference in electron screening for the $Tb^{3+}$ and $Y^{3+}$ ions and the Dzyaloshinski–Moriya off-diagonal exchange for which $D/J_0 \approx 0.1$ [8, 10]. The point is that the expected RMA is *weak*, as a good many experiments confirm [8]. Perhaps it is worthwhile to comment that the mere partial substitution of Tb by another RE with different anisotropy would not give a fully random easy direction distribution, and moreover the anisotropy would not be weak.

In weak RMA systems when the condition $H_{ex} \gg H > H_{RMA}$ is fulfilled, where $H_{ex}(= CJJ_0(a/R_a)^2/g\mu_B)$ is the effective exchange field and $H_{RMA}(= 4JD/g\mu_B)$ the RMA one [11], one has a *ferromagnet of wandering axis* (FWA), where long-range ferromagnetic order (LRFO) along the applied field $\boldsymbol{H}$ is formed, but the transverse ferromagnetic order is limited to distances $R_\perp = (H_{ex}/H)^{1/2}R_a$ [11, 12]. $R_a$ is the structural correlation length, $a$ the nearest-neighbour distance and $C$ a constant approximately equal to

unity. Hence no overall LRFO is developed, as was predicted for spatial dimension $d < 4$ [13], although $R_\perp$ can be substantial.

## 2. Experimental details

The pseudobinary C-15 Laves phase cubic intermetallics $Tb_xY_{1-x}Al_2$ (nominally $0.25 < x < 1.00$) were prepared by argon arc melting from their constituents, aluminium of 99.999% and terbium and yttrium of 99.9% purities. The melted buttons were remelted several times in order to attain good homogeneity and annealed at 900 °C for 1 week in high vacuum ($4 \times 10^{-6}$ mbar). Powder x-ray diffraction showed that the structure was the Laves phase C-15 one. The measured lattice parameters, using the extrapolation Nelson–Riley technique, were in between the parameters for $TbAl_2$ and $YaAl_2$ [14]. The existence of secondary phases was investigated using scanning electron microscopy (SEM) in the electron backscattered mode, and no foreign phases were detected. The chemical compositions were determined by SEM x-ray energy dispersion fluorescence, the measured compositions being $x = 0.24$, 0.48, 0.59, 0.87 and 1.0. Within this work also a single crystal of $TbAl_2$ was investigated; it was grown using the Czochralsky technique, the sample having the form of a cylinder 6 mm in diameter by 1 mm in thickness, with the cylinder basis coinciding with the (110) plane. In order to avoid the effect on the measured magnetization of a possible grain preferential orientation, we cut the samples in the form of a disc with its plane perpendicular to the button cooling axis after the melting. The magnetization was measured within this plane.

Magnetization measurements were performed, using a commercial VSM, between 4 K and well above the $T_{CSG}(x)$ boundary, i.e. the temperatures where the transitions from paramagnetic to CSG structure occur [8]. The applied magnetic fields were between $\cong 0$ and 12 T, produced with a superconducting solenoid. The accuracy of the measured magnetic moments was $\pm 5 \times 10^{-6}$ emu. The magnetostriction measurements were performed in the same ranges of temperature and field, using the well known strain-gauge technique, the sensitivity being $\pm 5 \times 10^{-7}$. Great care was exercised in the calibration of the gauge factor at the lowest temperatures of measurement. The calibration was performed by using the well known thermal expansion of a copper sample (purity 99.999%) against pure fused silica, for which the thermal expansion coefficient is comparatively negligible ($\cong 5 \times 10^{-7}$–$5 \times 10^{-6}$ $K^{-1}$). The magnetostriction was measured in directions parallel, $\lambda_\parallel$, and perpendicular, $\lambda_\perp$, to the applied magnetic field, in order to determine the linear or anisotropic striction, i.e. $\lambda_2 = \lambda_\parallel - \lambda_\perp = (3/2)(\lambda_\parallel - \omega/3)$, where $\omega$ is the volume strain. In figures 1 and 2 we respectively present the magnetization and magnetostriction isotherms for the compound $Tb_{0.59}Y_{0.41}Al_2$, which is quite representative of the studied compounds, where we can see that neither the magnetization nor the magnetostrictions saturate at the lowest temperature even at 12 T (see also figure 3 for the 4 K magnetization isotherms of the studied compounds).

## 3. A magnetostriction spin wave model for weak random magnetic anisotropy systems

Our magnetostriction spin wave (s.w.) model [6] deals with the magnetization dependence of $\lambda_2$ for weak RMA systems within the FWA regime (see section 1), i.e. for a system quasisaturated under a sufficiently strong applied magnetic field. The crucial difference from magnetically well ordered systems is that because of the structural disorder the thermal

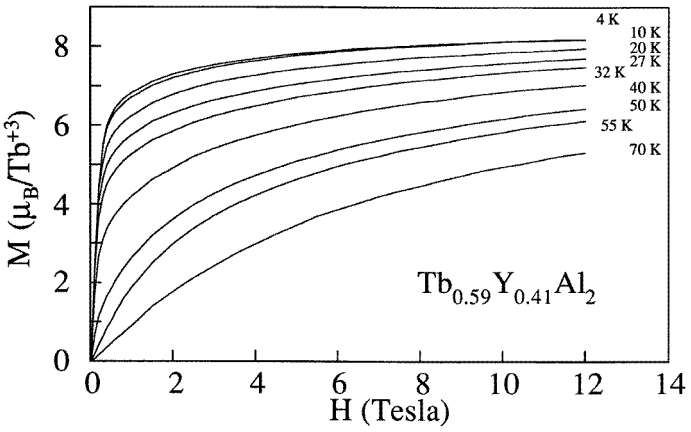


**Figure 1.** Magnetization isotherms against applied magnetic field for the intermetallic compound $Tb_{0.59}Y_{0.41}Al_2$.

averages $\langle J_z\rangle_T$ and $\langle Y_n^0(\boldsymbol{J})\rangle_T$ (see section 1) should now include the average over the disorder of the random easy axis distribution, $\langle\cdots\rangle_c$, and therefore $\lambda_2(T,H)/\lambda_2(0,H)$ and $m(T,H)$ will adopt the forms

$$\lambda_2(T,H)/\lambda_2(0,H) = \langle\langle Y_2^0(\boldsymbol{J})\rangle_T\rangle_c/\langle Y_2^0(\boldsymbol{J})\rangle_c \qquad m(T,H) = \langle\langle J_z\rangle_T\rangle_c/\langle J_z\rangle_c. \tag{4}$$

We have elsewhere [11] developed in full detail an s.w. model for weak RMA systems within the FWA regime (see section 1), which we will briefly outline here, in order to understand the main points of the s.w. magnetostriction model. The main purpose of such a presentation is to introduce the diagonalization transformations followed with Hamiltonian (3), which are needed in order to calculate $\lambda_2(T,H)$. In fact in order to perform such a diagonalization it is convenient to work in the magnon space. For such a purpose, we express the angular momentum operators $J_l^z$, $J_l^+$ and $J_l^-$ in terms of the site spin deviation operators $a_l^+$ and $a_l^-$, which in turn are transformed to creation and annihilation magnon operators $a_{\boldsymbol{k}}^+$ and $a_{\boldsymbol{k}}^-$ respectively, of wavevector $\boldsymbol{k}$. In this way we obtain the following Hamiltonian [11]:

$$H = \sum_{\boldsymbol{k}} \epsilon(\boldsymbol{k}) a_{\boldsymbol{k}}^+ a_{\boldsymbol{k}} - \frac{SD}{\sqrt{N}} \sum_{\boldsymbol{k},\boldsymbol{k}'} \{-Y_{20}(\boldsymbol{k}'-\boldsymbol{k}) a_{\boldsymbol{k}}^+ a_{\boldsymbol{k}'} + Y_{22}(-\boldsymbol{k}-\boldsymbol{k}') a_{\boldsymbol{k}}^+ a_{\boldsymbol{k}'}\}$$
$$-\sqrt{2}S^{3/2} D \sum_{\boldsymbol{k}} (Y_{20}^+(-\boldsymbol{k}) a_{\boldsymbol{k}}) + \text{CC} \tag{5}$$

where $\epsilon(\boldsymbol{k}) = Ak^2 + g_J\mu_B H$ is the unperturbed magnon energy, with an s.w. stiffness constant $A = C' J_0 S a^2$, where $S = (g_J - 1)J$ is the spin quantum number, $a$ the lattice constant and $C'$ a constant depending on the crystalline structure. The terms $Y_{20}(\boldsymbol{k}'-\boldsymbol{k})$, $Y_{22}(-\boldsymbol{k}-\boldsymbol{k}')$ and CC are the Fourier transforms of the complex spherical harmonics $Y_{nm}(\hat{\boldsymbol{a}}_l)$ [11]. The Hamiltonian (5) is of the Holstein–Primakoff type but differs from it in the terms linear in $a_{\boldsymbol{k}}^+$ and $a_{\boldsymbol{k}}$ and in the non-diagonal terms within the curly brackets. These last terms take into account the scattering suffered by the s.w. from the crystal field of random easy axis $\hat{\boldsymbol{a}}_l$. It was shown [11] that the linear terms are removed by the diagonalization transformations

$$a_{\boldsymbol{k}} = \alpha_{\boldsymbol{k}} + c_{\boldsymbol{k}} \text{ and CC} \tag{6}$$

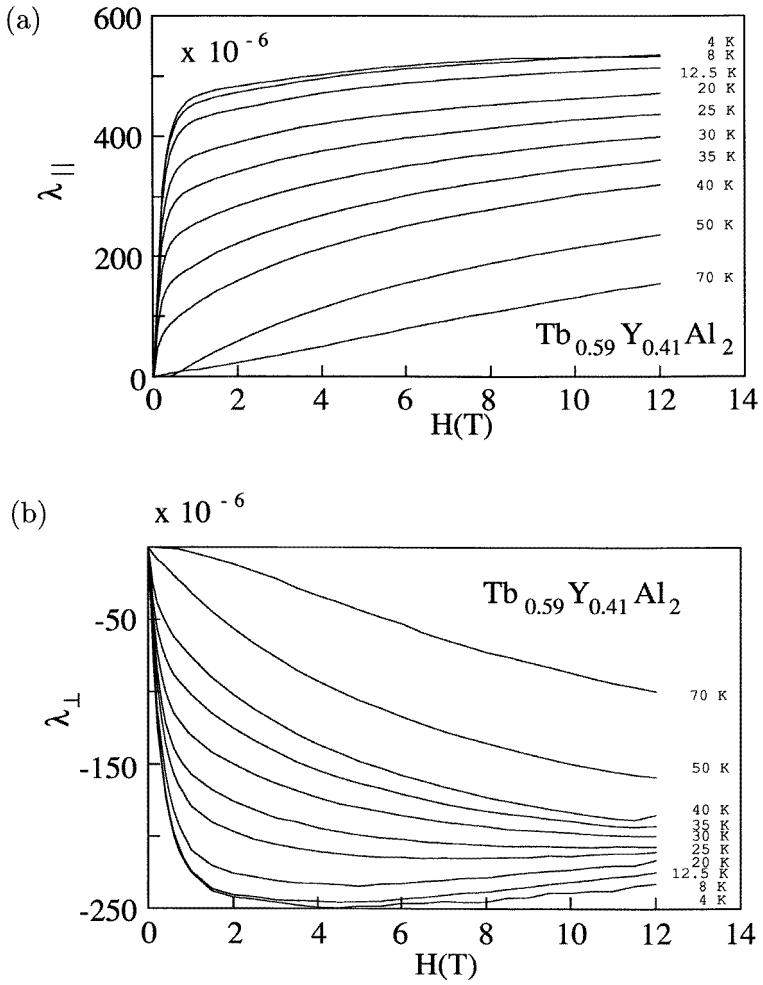


**Figure 2.** Magnetostriction isotherms for the compound $Tb_{0.59}Y_{0.41}Al_2$: (*a*) parallel ($\lambda_\parallel$) to the applied magnetic field, $\boldsymbol{H}$; (*b*) perpendicular ($\lambda_\perp$) to $\boldsymbol{H}$.

where $\alpha_k$ and $\alpha_k^+$ are boson operators and $c_k$ are *c*-numbers. A second transformation is required to fully diagonalize Hamiltonian (5), of the form [11]

$$\alpha_k = \beta_k + \sum_{k'}(u_{kk'}\beta_{k'} + v_{kk'}\beta_{k'}^+) \text{ and CC.} \tag{7}$$

The form of the matrices $u_{kk'}$ and $v_{kk'}$ can be found elsewhere [11], and $\beta_k$ and $\beta_k^+$ are again boson operators.

It can be easily shown that the crystal space transformations diagonalizing Hamiltonian (3) are the ones obtained by Fourier transforming jointly (6) and (7). In this way we obtain

$$a_l = (1 + u_l)\alpha_l + v_l\alpha_l^+ + c_l \text{ and CC} \tag{8}$$

where $\alpha_l$, $\alpha_l^+$ are dynamic boson operators, $c_l$, $c_l^+$, static disorder spin deviation *c*-numbers and $u_l$ and $v_l$ the Fourier transforms of the matrices $u_{kk'}$ and $v_{kk'}$. These matrices again account for the dynamical s.w. scattering by the RMA disorder. The particular expressions

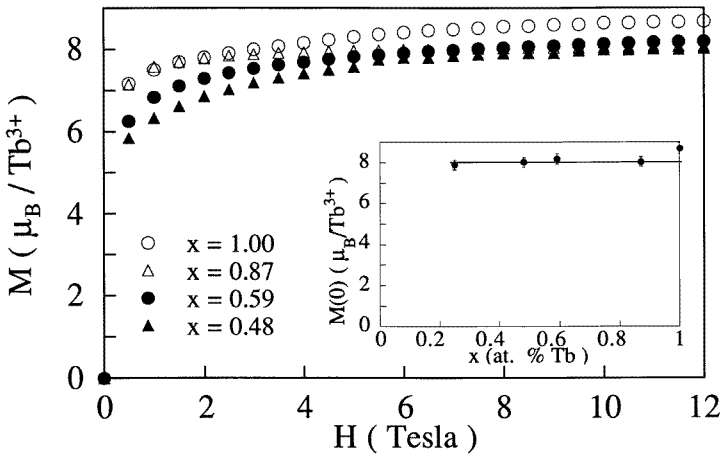


**Figure 3.** Low-temperature (4 K) magnetization isotherms for the polycrystalline $Tb_xY_{1-x}Al_2$ compounds, within the correlated spin glass regime of the magnetic phase diagram. Inset, the Tb concentration, $x$, dependence of the 0 K extrapolated 'saturation' ($H = 12$ T) magnetic moment for this series of compounds.

for all of these matrices and operators are not needed here in order to obtain the required relation between $\lambda_2(T, H)/\lambda_2(0, H)$ and $m(T, H)$ and they will be skipped. In fact we can write

$$M(T, H)/gJ\mu_B = 1 - J^{-1}\langle\langle a_l^+ a_l\rangle_T\rangle_c \tag{9}$$

and by use of (8) the 0 K magnetization becomes

$$M(0, H)/gJ\mu_B = 1 - J^{-1}\{\langle c_l^+ c_l\rangle_c + \langle v_l^+ v_l\rangle_c\}. \tag{10}$$

Also,

$$\langle\langle Y_2^0(\boldsymbol{J})\rangle_T\rangle_c = 3J^2 - J(J+1) - 3(2J-1)\langle\langle a_l^+ a_l\rangle_T\rangle_c + 3\langle\langle a_l^+ a_l^+ a_l a_l\rangle_T\rangle_c. \tag{11}$$

Then from (9) and (11) we readily obtain

$$\begin{aligned}\langle\langle Y_2^0(\boldsymbol{J})\rangle_T\rangle_c = {} & 3J^2 - J(J+1) - 3J(2J-1)(1-(gJ\mu_B)^{-1}M(T, H)) \\ & +6J^2(1-(gJ\mu_B)^{-1}M(T, H))^2\end{aligned} \tag{12}$$

where the last term in (12) originates from the decoupling of the quartic term in (11), i.e.

$$\langle\langle a_l^+ a_l^+ a_l a_l\rangle_T\rangle_c = 2\langle\langle a_l^+ a_l\rangle_T\rangle_c^2 \tag{13}$$

which seems in principle a good enough approximation when $H \ll H_{ex}$, as proved in [11].

The important result issuing from (12) is the possibility of expressing $\langle\langle Y_2^0(\boldsymbol{J})\rangle_T\rangle_c$ and $\langle Y_2^0(\boldsymbol{J})\rangle_c$ only in terms of $J$ and $M(T, H)$ and $M(0, H)$ respectively, and hence $\lambda_2$. In fact from (9), (10) and (12) it is easy to arrive at the expression

$$\frac{\lambda_2(T, H)}{\lambda_2(0, H)} = \frac{2J-1-3(2J-1)(1-(g_J\mu_B J)^{-1}M(T, H))+6J[1-(g_J\mu_B J)^{-1}M(T, H)]^2}{2J-1-3(2J-1)(1-(g_J\mu_B J)^{-1}M(0, H))+6J[1-(g_J\mu_B J)^{-1}M(0, H)]^2}. \tag{14}$$

If we perform the quotient (14) at temperatures low enough that we can take $M(T, H) \cong M(0, H)$, it can be easily shown that

$$\lambda_2(T, H)/\lambda_2(0, H) = 1 - 3\xi(1 - m(T, H)) \cong m(T, H)^p \tag{15}$$

with the Zener-like exponent $p$ given by

$$p = 3\xi = 3\frac{J(2J-1) - 6J\delta + \delta(1+4\delta)}{J(2J-1) - 6J\delta + 3\delta(1+2\delta)} \tag{16}$$

where

$$\delta = J\Delta m(0, H) \qquad \Delta m(0, H) = (gJ\mu_B)^{-1}\,\Delta M(0, H) = 1 - (gJ\mu_B)^{-1}M(0, H). \tag{17}$$

Therefore, according to (15), for weak RMA systems under the FWA regime, a Zener-like power law for the linear magnetostriction is predicted.

The 0 K reduced magnetization quantum defect is a consequence of the static spin deviations and s.w. scattering produced by the RMA disorder, according to (10). Therefore the important prediction is that for $\Delta M(0, H) \neq 0$ and at low enough temperatures the exponent $p$ is *smaller* than three, i.e. a violation of the $m^3$ Zener law occurs. Notice that for $\Delta M(0, H) = 0$ the $m^3$ power is regained. Also, for fixed $J$, $p$ decreases monotonically when $\Delta m(0, H)$ increases, as we can see in figure 4, where we present the variation of $p$ with $\Delta m(0, H)$ for the $Tb^{3+}$ ion ($J = 6$).

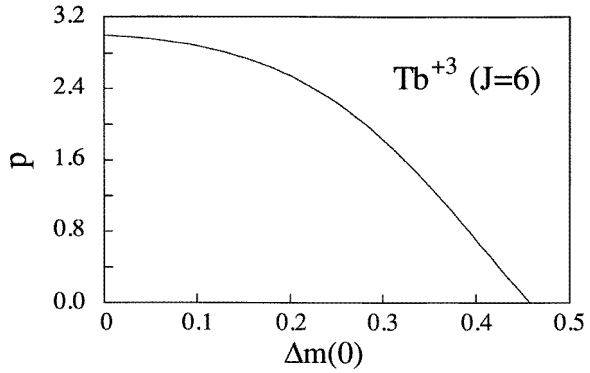


**Figure 4.** The theoretical dependence of the Zener-like exponent $p$ against the 0 K reduced magnetization defect $\Delta m(0)$ for the $Tb^{3+}$ ion.

## 4. Results and comparison with model predictions

We have observed, for the first time, the above predicted violation of the $m^3$ Zener law in the intermetallics $Tb_xY_{1-x}Al_2$. Two previous results should be reported. In the inset of figure 3 we show the extrapolated 0 K values for the measured 12 T 'saturation' magnetization. For the good ferromagnet $TbAl_2$ the measured moment (at 4 K and 12 T) in a polycrystalline sample is $(8.7 \pm 0.2)\ \mu_B$, within the experimental error very close to the unquenched free moment $\mu_{Tb^{3+}} = gJ\mu_B = 9\mu_B$. This result is corroborated by the spontaneous magnetic moment determined in a $TbAl_2$ single crystal, along the $\langle 111 \rangle$ easy direction, obtaining $(9.0 \pm 0.2)\ \mu_B$ from the extrapolation down to $H = 0$ of the 4 K magnetization isotherm, as shown in figure 5. On the other hand for $0.24 \leqslant x \leqslant 0.87$ the moments are reduced down to a constant value of $(8.0 \pm 0.2)\ \mu_B$ (see the inset of figure 3). Moreover, for a ferromagnet the expected single-crystal (cr.) magnetization value at remanence, obtained from the polycrystalline (pol.) value, is given by $\mu(\text{cr.}) = \mu(\text{pol.})/0.866$ [15]. For $TbAl_2$, this relation yields, from the 4 K remanence value of $(8.0 \pm 0.2)\ \mu_B$ (see figure 3), $\mu(\text{cr.}) = (9.2 \pm 0.2)\ \mu_B$, signalling no CEF quenching again. The overall conclusion

is that for $x < 1$ the observed $\Delta M(0, H)$ reduction is not a uniform CEF quenching effect, but a static RMA disorder quantum effect. Therefore the $Tb_xY_{1-x}Al_2$ series is a good testing ground for observation of the predicted $m^3$ magnetostriction law violation.

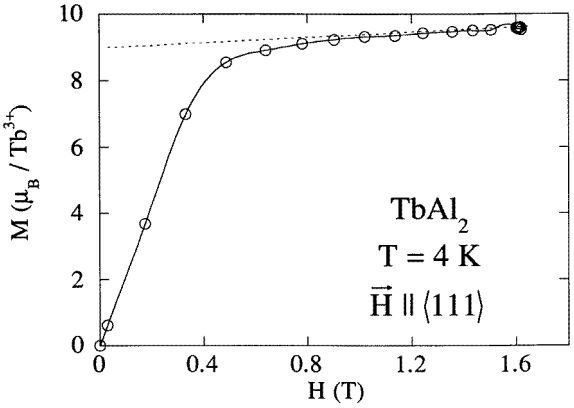


**Figure 5.** The magnetization isotherm at 4 K for applied magnetic field along the easy direction ⟨111⟩ for a $TbAl_2$ single crystal. The dashed line is the zero-field magnetization extrapolation.

Also important is to decide the range of magnetic fields, $H$, to apply in order to obtain the FWA regime. From the observation of the 4 K magnetization isotherms of figure 3, the effective anisotropy field, $H_k$, can be estimated from the curve knees and therefore taken as $H_k \cong 0.5$ T. The FWA regime will be reached if $H > H_k$, but $H$ should not be too much higher because the FWA regime would be severely distorted or even destroyed [11]. We chose a compromise, taking $H = 3$ T, in order to compare with our model results. In figure 6 we present the 3 T magnetization isofields, at the CSG regime of the magnetic phase diagram, and in figure 7 the $\lambda_2$ magnetostriction isofields at 3 T as well.

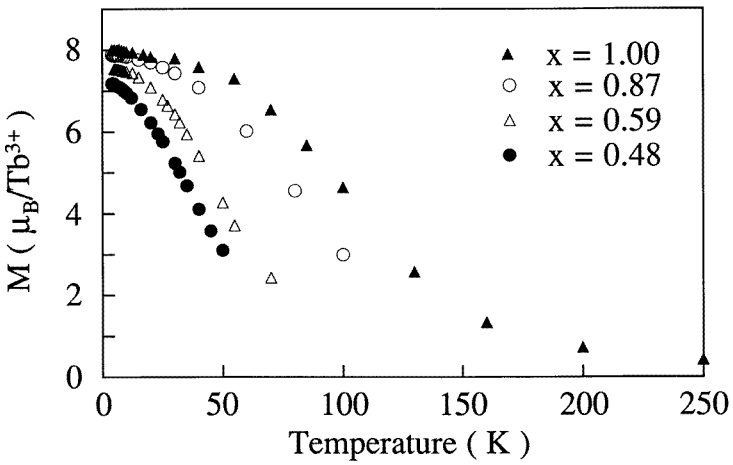


**Figure 6.** Magnetization isofields at $H = 3$ T for $Tb_xY_{1-x}Al_2$ compounds, within the correlated spin glass regime of the magnetic phase diagram.

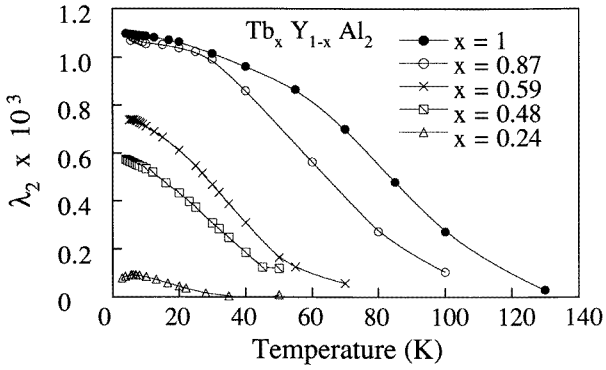


**Figure 7.** As figure 6, but for the second-order linear magnetostriction, $\lambda_2$.

In figure 8, we present the double-logarithmic plots of $\lambda_2(T, H = 3\ \mathrm{T})$ against $M(T, H = 3\ \mathrm{T})$, obtaining good linear relations for temperatures well below $T_{CSG}(x)$; the slopes are the $p$ exponents. The exponents $p$ have been plotted against $x$ in the inset of figure 8. For $TbAl_2$, $p = 3.0 \pm 0.15$, but for Tb concentrations $x < 1$ they are substantially *smaller* than three, in excellent agreement with our model prediction.

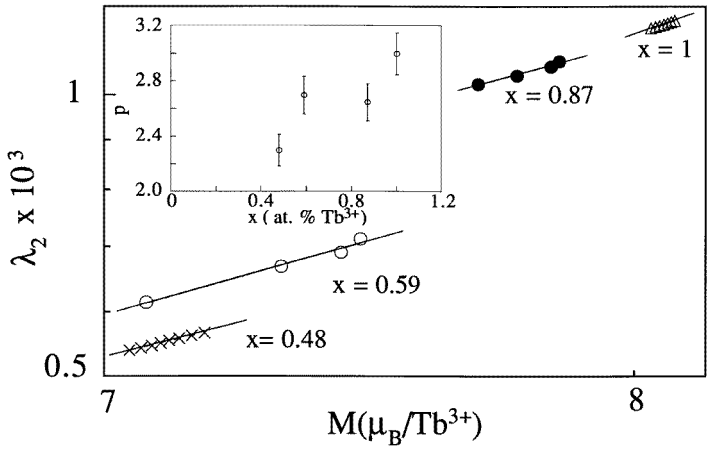


**Figure 8.** A double-log plot of the second-order linear magnetostriction, $\lambda_2$, against the magnetization (use of reduced units as in (15) is irrelevant), at both $H = 3$ T and temperatures below the P–CSG boundary. Lines are linear fits. Inset, Zener-like exponent, $p$, against Tb concentration, $x$, for $\lambda_2$, at an applied field $H = 3$ T.

As we signalled before we expect that at high enough applied fields $\boldsymbol{H}$ the FWA will approach a 3D Heisenberg ferromagnet, parallel to $\boldsymbol{H}$. This is, in fact, what happens, as we show in figure 9, where at 12 T, for the compound $x = 0.87$, $p = 3.1 \pm 0.15$, with $p = 2.9 \pm 0.15$ and $2.7 \pm 0.15$ for $x = 0.59$ and 0.48 respectively, due to the increasing RMA strength $D$.

A good consistency check of our results is to compare the measured $p$-values with the theoretically predicted values, as shown in figure 4. To do this, in figure 10 we have plotted $p$ at 3 T against the experimental magnetization quantum defect at 3 T as well, as

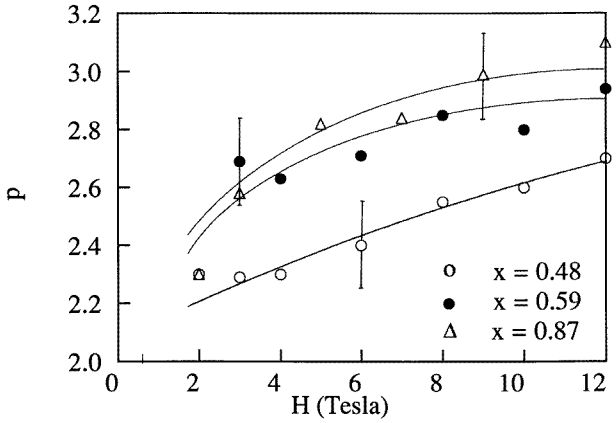


**Figure 9.** The magnetic field dependence of the Zener-like exponent, $p$, for $Tb_xY_{1-x}Al_2$ compounds, with $x = 0.48$, 0.59 and 0.87. The lines are guides for the eye.

obtained in the following way. Looking at the magnetization isotherms of figure 3 or at the isofields of figure 6, we notice that at 3 T the magnetization for polycrystalline $TbAl_2$ is smaller than the spontaneous value of $(9.0 \pm 0.2)\ \mu_B$, as obtained above. This lack of saturation is probably due to the grain distribution misalignment, an effect that should probably also be present for the compounds with $x < 1$. This means that in order to calculate the magnetization *quantum* defect for $x < 1$ at 3 T we must take as reference the magnetization of polycrystalline $TbAl_2$ at the same field. Changing $gJ\mu_B$ for this value in the second of equations (17), we obtain for $\Delta m(0, 3\ \mathrm{T})$ the values quoted in figure 10. As we can see the decrease of $p$ with $\Delta m(0, 3\ \mathrm{T})$ is faster than the theoretical prediction. This indicates that more theoretical work beyond the simple model here presented is needed. A possibility for such disagreement is that the decoupling in (13) is not accurate enough.

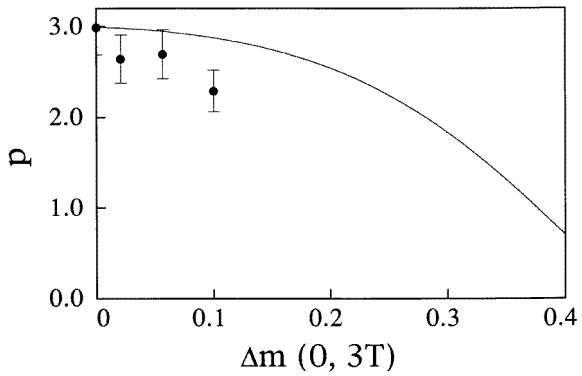


**Figure 10.** Variation of the Zener-like $p$ exponent with the reduced magnetization defect at 0 K and 3 T. The points (●) are the experimental values at 3 T and the line the theoretical prediction.

## 5. Conclusions

In conclusion, we have shown that for crystalline weak random anisotropy magnets, in the quasisaturated regime, the well established low-temperature magnetostriction $m^3$ Zener law is clearly violated, as a consequence of the 0 K magnetization quantum reduction due to the static spin deviations and 0 K s.w. scattering. It should be emphasized that because weak RMA does not disturb the assumed cylindrical symmetry around the average magnetization vector, $\boldsymbol{M}$, direction, the relationship $\lambda_n \sim m^p$ between the linear magnetostriction, $\lambda_n$, and the reduced magnetization, $m$, is preserved, although the Zener exponent, $p$, is severely reduced from the value $n(n+1)/2$. This apparently is a consequence of the $\Delta M(0, H)$ reduction, which in turn requires a reduction of $p$, if spin cylindrical symmetry around $\boldsymbol{M}$ is essentially preserved in the FWA regime over the transverse correlation length, $R_\perp$.

## Acknowledgments

AdM is grateful to J Cullen (NSWC, Washington) who was coauthor of the early version of the model which motivated this research. We are grateful to S J Abell (University of Birmingham) for growing the $TbAl_2$ single crystals. The financial support of the Spanish DGICYT under grants PB91/0936 and PB93/0584, and of the EU under grants CHRX-CT93/0352 and BE3039/89, is gratefully acknowledged.

## References

[1] Zener C 1954 *Phys. Rev.* B **96** 1335
Akulov N 1936 *Z. Phys.* **100** 197
Callen E and Callen H B 1963 *Phys. Rev.* **129** 578
[2] Callen E and Callen H B 1965 *Phys. Rev.* **139** A455
[3] Callen E 1982 *J. Appl. Phys.* **53** 8139
[4] Callen H B and Shtrikman S 1965 *Solid State Commun.* **3** 5
[5] For transition metal amorphous alloys see e.g. de Lacheisserie E T 1993 *Magnetostriction—Theory and Applications of Magnetoelasticity* (Boca Raton, FL: Chemical Rubber Company); for rare earth based ones see e.g. del Moral A, Ibarra M R, Algarabel P A and Arnaudas J I 1991 *Physics of Magnetic Materials* ed W Gorzkowski, M Gutowski, H K Lachowicz and H Szymczak (Singapore: World Scientific), p 204
del Moral A 1993 *Magnetoelastic Effects and Applications* ed L Lanotte (Amsterdam: Kluwer) p 1
[6] Cullen J R and del Moral A 1990 *J. Magn. Magn. Mater.* **83** 157
[7] Purwins H G, Walker E, Barbara B and Rossignol M F 1973 *Phys. Lett.* **45A** 427
Abell J S, del Moral A, Ibarra M R and Lee E W 1983 *J. Phys. C: Solid State Phys.* **16** 769
[8] del Moral A, Arnaudas J I, de la Fuente C, Ciria M, Joven E and Gehring P M 1994 *J. Appl. Phys.* **76** 6180
Joven E, del Moral A and Arnaudas J I 1991 *J. Appl. Phys.* **69** 5069 and references therein
[9] Harris R, Plischke M and Zuckermann M J 1973 *Phys. Rev. Lett.* **31** 160
[10] Gehring P M, Salamon M B, del Moral A and Arnaudas J I 1990 *Phys. Rev.* B **41** 9134
[11] del Moral A and Cullen J 1995 *J. Magn. Magn. Mater.* **139** 39
[12] Chudnovky E M, Saslow W M and Serota R A 1986 *Phys. Rev.* B **33** 251
[13] Pelcovits R A, Pytte E and Rudnick J 1978 *Phys. Rev. Lett.* **40** 476
[14] Buschow K H J 1979 *Rep. Prog. Phys.* **42** 1373
[15] Chikazumi S 1964 *Physics of Magnetism* (New York: Wiley) p 251